

## Collective Path Connecting the Oblate and Prolate Local Minima in $^{68}\text{Se}$

Masato KOBAYASI,<sup>1</sup> Takashi NAKATSUKASA,<sup>2</sup> Masayuki MATSUO<sup>3</sup>  
and Kenichi MATSUYANAGI<sup>1</sup>

<sup>1</sup> *Department of Physics, Graduate School of Science,  
Kyoto University, Kitashirakawa, Kyoto 606-8502, Japan*

<sup>2</sup> *Institute of Physics and Center for Computational Science, University of Tsukuba,  
Tsukuba 305-8571, Japan*

<sup>3</sup> *Graduate School of Science and Technology,  
Niigata University, Niigata 950-2181, Japan*

By means of the adiabatic self-consistent collective coordinate method and the pairing plus quadrupole interaction, we have obtained the self-consistent collective path connecting the oblate and prolate local minima in  $^{68}\text{Se}$  for the first time. Result of calculation indicates importance of triaxial deformation dynamics in the oblate-prolate shape coexistence phenomena.

Shape coexistence phenomena are typical examples of large amplitude collective motion in nuclei. These phenomena imply that different solutions of the Hartree-Fock-Bogoliubov (HFB) equations (local minima in the deformation energy surface) appear in the same energy region and that the nucleus exhibits large amplitude collective motion connecting these different equilibrium points. The identities and mixings of these different shapes are determined by the dynamics of such collective motion. Some years ago, we have proposed a new method of describing such large-amplitude collective motion, which is called Adiabatic Self-Consistent Collective Coordinate (ASCC) method.<sup>1)</sup> It yields a new method of solving the basic equations of the SCC method<sup>2)</sup> using an expansion in terms of the collective momentum. It does not assume a single local minimum, so that it is expected to be suitable for the description of the shape coexistence phenomena. The ASCC method also enables us to include the pairing correlations self-consistently, removing the spurious number fluctuation modes. To examine the feasibility of the ASCC method, we have first applied it to an exactly solvable model called the multi- $O(4)$  model, which is a simplified version of the pairing-plus-quadrupole (P+Q) interaction model.<sup>3)</sup> It is shown that the method yields a faithful description of tunneling motion through a barrier between the prolate and oblate local minima in the collective potential.<sup>4)</sup>

In this Letter, we give a brief report of our first application of the ASCC method to a realistic P+Q interaction model. We illustrate its practicality taking as a typical example the oblate-prolate shape coexistence phenomenon in  $^{68}\text{Se}$  recently observed in experiments.<sup>5)</sup> The self-consistent collective path obtained successfully by means of the ASCC method is found to run approximately along the valley connecting the oblate and prolate local minima in the collective potential energy landscape. To the best of our knowledge, this is the first time that a self-consistent collective

path is obtained for realistic situation starting from the microscopic P+Q Hamiltonian. We note that a similar approach to large amplitude collective motions was recently pursued by Almeded and Walet,<sup>6)</sup> although they discussed different nuclei and encountered some difficulties in obtaining self-consistent collective paths.

We assume that large-amplitude collective motions are described by a set of time-dependent HFB state vectors  $|\phi(q, p, \varphi, N)\rangle$  parametrized by a single collective coordinate  $q$ , the collective momentum  $p$  conjugate to  $q$ , the particle number  $N$  and the gauge angle  $\varphi$  conjugate to  $N$ . As discussed in Ref. 1), the state vector can be written

$$|\phi(q, p, \varphi, N)\rangle = e^{-i\varphi\hat{N}} |\phi(q, p, N)\rangle = e^{-i\varphi\hat{N}} e^{ip\hat{Q}(q)} |\phi(q)\rangle. \quad (1)$$

Making an expansion with respect to  $p$  and requiring that the time-dependent variational principle be fulfilled up to the second order in  $p$ , we obtain the following set of equations to determine  $|\phi(q)\rangle$ , the infinitesimal generator  $\hat{Q}(q)$ , and its canonical conjugate  $\hat{P}(q)$ :

$$\delta \langle \phi(q) | \hat{H}_M(q) | \phi(q) \rangle = 0, \quad (2)$$

$$\delta \langle \phi(q) | [\hat{H}_M(q), \hat{Q}(q)] - \frac{1}{i} B(q) \hat{P}(q) | \phi(q) \rangle = 0, \quad (3)$$

$$\delta \langle \phi(q) | [\hat{H}_M(q), \frac{1}{i} \hat{P}(q)] - C(q) \hat{Q}(q) - \frac{1}{2B(q)} [[\hat{H}_M(q), (\hat{H} - \lambda(q)\hat{N})_A], \hat{Q}(q)] - \frac{\partial \lambda}{\partial q} \hat{N} | \phi(q) \rangle = 0. \quad (4)$$

Here

$$\hat{H}_M(q) = \hat{H} - \lambda(q)\hat{N} - \frac{\partial V}{\partial q} \hat{Q}(q) \quad (5)$$

is the Hamiltonian in the moving frame;

$$C(q) = \frac{\partial^2 V}{\partial q^2} + \frac{1}{2B(q)} \frac{\partial B}{\partial q} \frac{\partial V}{\partial q} \quad (6)$$

is the local stiffness;  $(\hat{H} - \lambda\hat{N})_A$  represents the two-quasiparticle creation and annihilation parts of  $(\hat{H} - \lambda\hat{N})$ ;  $\hat{Q}(q)$  and  $\hat{P}(q)$  satisfy the canonical variable condition

$$\langle \phi(q) | [\hat{Q}(q), \hat{P}(q)] | \phi(q) \rangle = i. \quad (7)$$

Once  $|\phi(q)\rangle$  and the infinitesimal generators are determined for every values of  $q$ , we obtain the collective Hamiltonian  $\mathcal{H}(q, p) = \frac{1}{2}B(q)p^2 + V(q)$  with the collective potential  $V(q) = \langle \phi(q) | \hat{H} | \phi(q) \rangle$  and the inverse mass  $B(q) = -\langle \phi(q) | [[\hat{H}, \hat{Q}(q)], \hat{Q}(q)] | \phi(q) \rangle$ .

Table I. Spherical single-particle orbits and their energies used in the calculation. Energies relative to those of  $1g_{9/2}$  are written in MeV.

orbits	$1f_{7/2}$	$2p_{3/2}$	$1f_{5/2}$	$2p_{1/2}$	$1g_{9/2}$	$2d_{5/2}$	$1g_{7/2}$	$3s_{1/2}$	$2d_{3/2}$
protons	-8.77	-4.23	-2.41	-1.50	0.0	6.55	5.90	10.10	9.83
neutrons	-9.02	-4.93	-2.66	-2.21	0.0	5.27	6.36	8.34	8.80

We use the P+Q interaction model with the prescriptions of Ref. 3) for the microscopic Hamiltonian  $\hat{H}$ , but here the pairing and quadrupole force parameters are chosen as  $G = 0.320$  MeV (for both protons and neutrons) and  $\chi' = 0.248$  MeV so that the constrained HFB potential energy surface (shown by contour lines in Fig.1) exhibits two local minima at prolate and oblate shapes, whose pairing gaps, quadrupole deformation and energy difference approximately reproduce those obtained in a recent Skyrme-HFB calculation by Yamagami *et al.*<sup>7)</sup> The spherical single-particle energies are taken from those of the modified oscillator model of Ref. 8) and listed in Table I. In this way the effective Hamiltonian provides a suitable situation with which shape coexistence dynamics can be studied, although further improvements, *e.g.*, by including the quadrupole pairing and/or neutron-proton pairing interactions, may better be taken into account for quantitative comparison with experimental data.

We have used the following algorithm to solve the set of ASCC equations (2), (3), (4) and (7). Let the state vector  $|\phi(q)\rangle$  be known at a specific value of  $q$ . We first solve the local harmonic equations in the moving frame (the moving frame RPA), (3) and (4), under the condition (7) to obtain  $\hat{Q}(q)$  and  $\hat{P}(q)$ . This is done by a straightforward extension of the procedure described in Ref. 4). We then construct a state vector at the neighboring point  $q + \delta q$  by using the infinitesimal generator  $\hat{P}(q)$  as

$$|\phi(q + \delta q)\rangle = e^{-i\delta q \hat{P}(q)} |\phi(q)\rangle, \quad (8)$$

and solve the moving frame RPA with respect to this state to obtain  $\hat{Q}(q + \delta q)$  and  $\hat{P}(q + \delta q)$ . Though the above  $|\phi(q + \delta q)\rangle$  does not necessarily satisfy the HFB equation in the moving frame (2), we can use this state vector as an initial solution of (2) at  $q + \delta q$ . We search for the solution of (2) under the constraints

$$\langle \phi(q + \delta q) | \hat{N} | \phi(q + \delta q) \rangle = N, \quad (9)$$

$$\langle \phi(q + \delta q) | \hat{Q}(q) | \phi(q + \delta q) \rangle = \delta q \quad (10)$$

by means of the gradient method. Here the nucleon-number constraint (9) is actually applied for both proton and neutron numbers. Equation (10) is the constraint for the increment  $\delta q$  of the collective coordinate. After finding a solution of Eq. (2), we renew  $\hat{Q}(q + \delta q)$  and  $\hat{P}(q + \delta q)$  by solving again the moving frame RPA equations, (3) and (4), for the new state vector  $|\phi(q + \delta q)\rangle$  obtained above. Then we again solve Eq. (2) with the renewed  $\hat{Q}(q + \delta q)$ . If the above iterative procedure converges, we get the selfconsistent solutions that satisfy Eqs. (2), (3), (4) and (7) simultaneously at  $q + \delta q$ , and we can proceed to the next point  $q + 2\delta q$ . In actual numerical calculation, we start the procedure from one of the HFB local minimum and examine whether we arrive at the other local minimum by going along the collective path obtained above. We have checked that the same collective path is obtained by starting from the other local minimum and proceeding in an inverse way.

Carrying out the above procedure we have successfully obtained the collective path connecting the oblate and prolate local minima in <sup>68</sup>Se. The result is shown in Fig. 1. The deformation parameters  $\beta$  and  $\gamma$  are here defined as usual through the expectation values of the quadrupole operators.<sup>7)</sup> Roughly speaking, the collective

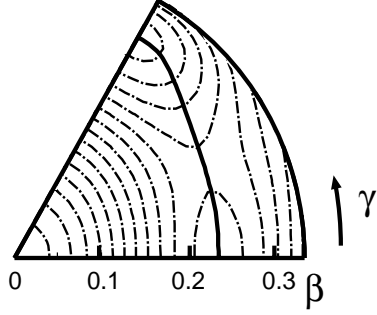


Fig. 1. The bold curve represents the ASCC path connecting the oblate and prolate minima in  $^{68}\text{Se}$  projected on the  $(\beta, \gamma)$  plane. The contour lines are calculated by the conventional constrained HFB method and plotted for every 100 keV.

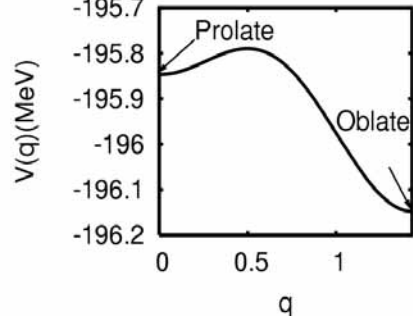


Fig. 2. Collective potential  $V(q)$  plotted as a function of the collective coordinate  $q$ . Here the origin of  $q$  is chosen to coincide with the prolate local minimum and its scale is defined such that the collective mass  $M(q) = 1 \text{ MeV}^{-1}$ .

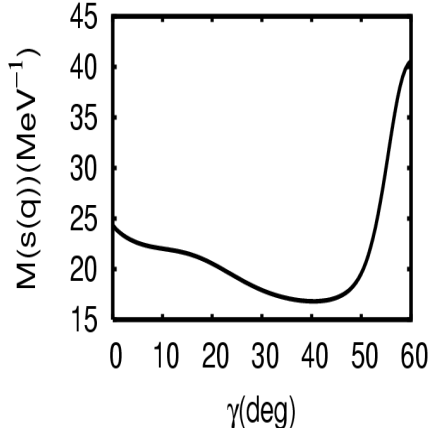


Fig. 3. Collective Mass  $M(s)$  with respect to the geometrical length  $s$  along the collective path in the  $(\beta, \gamma)$  plane is plotted as a function of the triaxiality parameter  $\gamma$ .

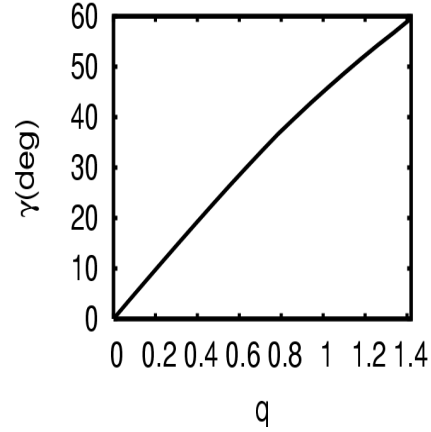


Fig. 4. The triaxiality parameter  $\gamma$  plotted as a function of the collective coordinate  $q$ .

path goes through the valley that exists in the  $\gamma$  direction and connects the oblate and prolate minima. If one treats the  $\beta$  as collective coordinate and connects the oblate and prolate shapes through the spherical point, variation of the potential energy would be much greater than that along the collective path we obtained. The potential energy curve  $V(q)$  along the collective path evaluated by the ASCC method is shown in Fig. 2. We have defined the scale of the collective coordinate  $q$  such that the collective mass  $M(q) = B(q)^{-1} = 1 \text{ MeV}^{-1}$ . The collective mass as a function of the geometrical length  $s$  along the collective path in the  $(\beta, \gamma)$  plane may be defined by  $M(s) = M(q)(ds/dq)^{-2}$  with  $ds^2 = d\beta^2 + \beta^2 d\gamma^2$ . This quantity is presented in Fig. 3 as a function of  $\gamma$ . The triaxial deformation parameter  $\gamma$  is plotted as a

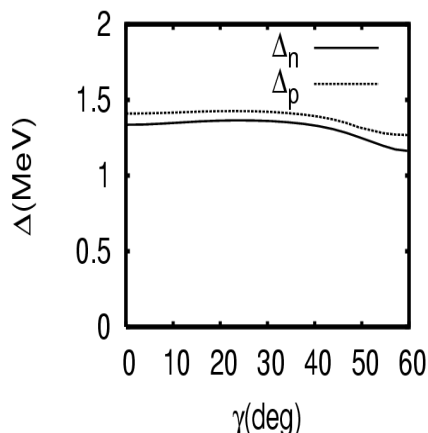


Fig. 5. Neutron and proton pairing gaps,  $\Delta_n$  and  $\Delta_p$ , plotted as functions of  $\gamma$ .

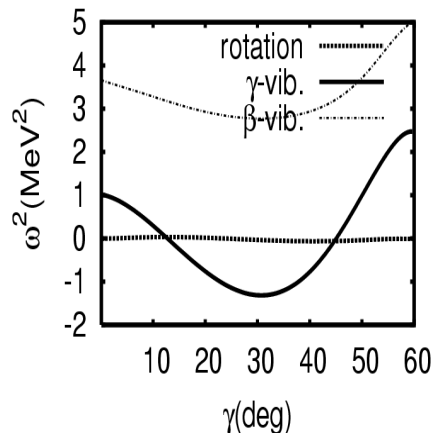


Fig. 6. Lowest three eigen-frequencies squared,  $\omega^2 = BC$ , of the moving frame RPA, plotted as functions of  $\gamma$ .

function of  $q$  in Fig. 4. Variations of the pairing gaps and of the lowest few eigen-frequencies of the moving frame RPA along the collective path are shown in Figs. 5 and 6. The solid curve in Fig. 6 represents the squared frequency  $\omega^2(q) = B(q)C(q)$ , given by the product of the inverse mass  $B(q)$  and the local stiffness  $C(q)$ , for the moving frame RPA mode that develops from the  $\gamma$ -vibration in the oblate and prolate limits and determines the infinitesimal generators  $\hat{Q}(q)$  and  $\hat{P}(q)$  along the collective path. The other two curves are solutions of the moving frame RPA having characters of the collective rotational motion and the  $\beta$ -vibration, which are however irrelevant to the collective path. Note that the frequency of the  $\gamma$  mode becomes imaginary in the region  $12^\circ < \gamma < 45^\circ$ . These results will reveal interesting dynamical properties of the shape coexistence phenomena in  $^{68}\text{Se}$ . For instance, the large collective mass in the vicinity of  $\gamma = 60^\circ$  (Fig. 3) might increase stability of the oblate shape in the ground state. Detailed discussions on these quantities as well as the solutions of the collective Schrödinger equation will be given in a forthcoming full-length paper.<sup>11)</sup>

In summary, we have applied the ASCC method to the oblate-prolate shape coexistence phenomena in  $^{68}\text{Se}$ . It was found that the collective path goes through the valley of the potential energy landscape in the  $(\beta, \gamma)$  plane along which the triaxial deformation parameter  $\gamma$  changes between  $0^\circ$  and  $60^\circ$  keeping the axially symmetric deformation parameter  $\beta$  approximately constant. This is the first time that a self-consistent collective path between the oblate and prolate minima is obtained for the realistic P+Q interaction model. Currently, the generator coordinate method has often been used to describe variety of shape coexistence phenomena taking the  $\beta$  as the generator coordinate.<sup>9)</sup> The triaxial shape vibrational degrees of freedom is ignored also in the extensive microscopic calculation of Ref. 10). The result of the ASCC calculation, however, strongly indicates the necessity of taking into account the  $\gamma$  degree of freedom at least for describing the oblate-prolate shape coexistence in  $^{68}\text{Se}$ . Effects of triaxial deformation dynamics on various properties of shape co-

existence, including results of calculation for neighboring nuclei, will be discussed in a full-length paper.<sup>11)</sup>

We thank Drs. D. Almeded and N. R. Walet for useful discussions and kindly pointing out a graphical error in the preprint version of this Letter. The numerical calculations were performed on the NEC SX-5 supercomputer at Yukawa Institute for Theoretical Physics, Kyoto University. This work was supported by the Grant-in-Aid for Scientific Research (Nos. 13640281, 14540250 and 14740146) from the Japan Society for the Promotion of Science.

- 
- 1) M. Matsuo, T. Nakatsukasa and K. Matsuyanagi, Prog. Theor. Phys. **103** (2000), 959.
  - 2) T. Marumori, T. Maskawa, F. Sakata and A. Kuriyama, Prog. Theor. Phys. **64** (1980), 1294.
  - 3) M. Baranger and K. Kumar, Nucl. Phys. **A110** (1968), 490.
  - 4) M. Kobayasi, T. Nakatsukasa, M. Matsuo and K. Matsuyanagi, Prog. Theor. Phys. **110** (2003), 61.
  - 5) S. M. Fischer *et al.*, Phys. Rev. Lett. **84** (2000), 4064; Phys. Rev. **C67** (2003), 064318.
  - 6) D. Almeded and N. R. Walet, Phys. Rev. **C69** (2004), 024302.
  - 7) M. Yamagami, K. Matsuyanagi and M. Matsuo, Nucl. Phys. **A693** (2001), 579.
  - 8) T. Bengtsson and I. Ragnarsson, Nucl. Phys. **A436** (1985), 14.
  - 9) T. Duguet, M. Bender, P. Bonche, and P.-H. Heenen, Phys. Lett. **B559** (2003), 201.
  - 10) A. Petrovici, K.W. Schmid, and A. Faessler, Nucl. Phys. **A710** (2002), 246.
  - 11) M. Kobayasi, T. Nakatsukasa, M. Matsuo and K. Matsuyanagi, in preparation.